Physica A 605 (2022) 127917

Contents lists available at ScienceDirect

Physica A

journal homepage: www.elsevier.com/locate/physa

Detecting limit cycles in stochastic time series

Emil S. Martiny, Mogens H. Jensen, Mathias S. Heltberg *

Department of Physics, University of Copenhagen, Denmark

ARTICLE INFO

Article history:
Received 9 January 2022
Received in revised form 23 June 2022
Available online 28 July 2022

Keywords:
Oscillations
Limit cycles
Stochastic dynamics
Statistical test

ABSTRACT

The emergence of oscillatory behaviour represents fundamental information about the interactions of the underlying system. In biological systems, oscillations have been observed in experimental data, but due to the significant level of noise, it is difficult to characterize whether observed dynamics based on time series, are truly limit cycles. Here, we present a simple three step method to identify the presence of limit cycles in stochastic systems. Considering input from one-dimensional time series, as are typically obtained in experiments, we propose statistical measures to detect the existence of limit cycles. This is tested on models from chemical networks, and we investigate how the underlying dynamics can be separated depending on the noise level and length of the series.

1. Introduction

The presence of oscillations is an important marker, observed in many biological systems [1–10]. In the past decades there has been growing evidence, that many of the most important regulatory proteins, known as transcription factors, exhibit oscillatory behaviour following external perturbations [11–24]. One particularly interesting example is the important protein p53, that exhibits oscillations in the nuclear concentration following a high dose of γ-radiation [25–28]. However, so far it has not been possible to make a decision on whether this behaviour is actually the result of a limit cycle, or whether this is the stochastic fluctuations that generate the oscillatory behaviour. Understanding the underlying network of these proteins is a key challenge to the field of systems biology, and therefore the precise identification of a Hopf bifurcation can be a very important element in the analysis and as a guidance in the model construction [29,30].

There is a large body of literature describing bifurcations in a variety of dynamical systems including the Hopf bifurcation, generally by using either maps [9,10], or invariant measures of the mathematical variables [31–35]. Applying techniques from these sources, we use the equilibrium distribution of the Fokker–Planck (FP) equation as an invariant measure, as a key tool to classifying the oscillatory behaviour. However we believe that there is a lack of applicability in the proposed methods, and our task is therefore to apply realistic series (similar to the ones extracted from experiments) and in a direct way proposes a tool that will lead to an understanding of the underlying systems and decipher the nature of oscillations.

Here, we outline a simple three-step method to analyse one-dimensional signals and decipher the origin of series that to the eye look like real oscillations. First, we transform the one dimensional series to a two dimensional distribution using time embedding. We then use Taylor expansion of the FP equation to obtain a general relation between the steady state probability distribution and the direction of the force on the trajectory close to the fixed point. Finally, we use this distribution to fit a curvature-parameter and based on the uncertainty in this parameter, we can quantify the likelihood

* Corresponding author.
E-mail address: Heltberg@nbi.ku.dk (M.S. Heltberg).

https://doi.org/10.1016/j.physa.2022.127917
0378-4371/

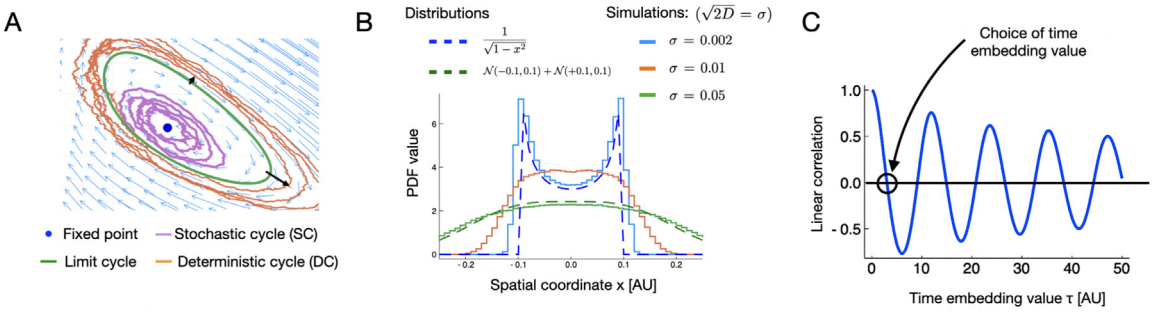

Fig. 1. (A) Schematic figure showing the phase space of oscillatory motion and the oscillatory dynamics in stochastic simulations of (1) a stochastic cycle (purple) and (2) a deterministic cycle (orange). (B) Schematic figure showing the probability distribution in one dimension for (1) small noise (blue), (2) medium noise (orange) and (3) large noise (green). Two probability distributions are shown for comparison. (C) Linear correlation of two data series as a function of the applied time delay τ. The arrow show the value we choose to generate the polar coordinates, when the linear correlation is equal to zero.

that the time signal stems from a limit cycle. To verify this, and show the applicability of the method, we test this on a series of chemical systems (with stochasticity similar to what is found in biological experiments) and estimate the rate of success for the method as a function of the parameter distance from the Hopf bifurcations, the levels of noise and the length of the time series. We believe that this work can be of great help and importance, to a broad audience doing research on dynamical protein networks [36].

2. Theory

We consider following the situation: In a laboratory, a long (or several short) time series have been measured. They exhibit oscillatory dynamics, but in order to extract knowledge from them, or include them in a mathematical model framework, we need to understand whether these oscillations show that the underlying system exhibit a stable limit cycle. Such systems can exhibit similar behaviour and therefore be difficult to distinguish (Fig. 1A).

In this section we derive how one can extract observables from the time series in order to determine the nature of the observed oscillations. We will use previously presented mathematical arguments, but since the main point of the article is to present an applicable method, we will point to references where the mathematical analysis is showed more rigorously.

Our aim is to determine whether oscillatory time series stems from a limit cycle in the underlying dynamical system (i.e. the system is above a Hopf bifurcation). We term this *true* Hopf bifurcation a deterministic cycle (DC). As an alternative, the system could have a fixed point, where the stochastic noise levels drive the system out of this point resulting in oscillatory dynamics with a well defined power spectrum [37,38]. In this case, the Jacobian matrix still possesses imaginary eigenvalues, but the real part of the eigenvalues is negative. We term this a stochastic cycle (SC), since the noise moves the system out of the stable fixed point.

Our approach is now to quantify the statistics for each of these systems and separate them based on hypothesis testing.

Time embedding is based on a data series $x(t)$, and a definition of a time embedded variable $x(t+\tau)$ where τ is a time delay. Therefore time embedding presents a way to include the history of information in the trajectories and is fundamentally based on Takens theorem which has been used in many studies of dynamical systems [39]. One basic property of the time embedding is that if $x(t)$ is periodic then $x(t+\tau)$ is periodic as well. Therefore we will use this to introduce two variables and thereby transform the time series into a two-dimensional phase space, spanned by $x(t)$ and $x(t+\tau)$. Theoretically, this works for all τ, but in practice we choose τ such that $x(t)$ and $x(t+\tau)$ are linearly uncorrelated, meaning the noise in the two dimensions is linearly uncorrelated as well. To obtain this, we choose τ by minimizing the absolute value of the linear correlation between a signal and itself shifted by some amount i.e. $x(t)$ and $x(t+\tau)$ (See Fig. 1(B)). This means that we increase the value of the time-delay until we reach a linear correlation of 0 for the first time. To get an intuition for this, one can consider the simple example of a $x(t) = sin(t)$ signal. Time embedding gives $(sin(t), sin(t+\tau))$, a time delay equal to of 1/4th of the period will clearly give $(sin(t), cos(t))$ - a circle, where the two coordinates are uncorrelated. Other choices of τ will result in ellipses. This use of uncorrelated data simplifies the derivations in the next step, and reduces the required amount of data.

The probability distribution of the radial coordinate, $P(r)$, represents the probability that the trajectory will be at a distance r from the centre of the cycle. With the constructed two-dimensional space from time embedding, we can empirically compute this distribution, but we will derive expressions for the theoretical model. Here we follow a scheme similar to one that has been presented in Refs. [31–35], but we propose to apply it directly to the empirical distribution instead of a system of equations. This is advantageous since it makes the method applicable when we do not know the equations leading to the observed dynamics.

Close to the Hopf bifurcation, a limit cycle takes an elliptic form, so $x(t)$ (one of the two coordinates) will be on the form:

$$x(t) = a\ cos(\omega t + \phi) = a\ cos(\theta) \tag{1}$$

where a is the amplitude of the oscillatory motion. This means that the velocity of this will be:

$$v(\theta) = -a\omega sin(cos^{-1}(\frac{x}{a})) = -a\omega\sqrt{1-(\frac{x}{a})^2} \tag{2}$$

If we now assume that the system is moving in the presence of stochastic, white noise, the resulting stochastic differential equation will take the form:

$$dx = dt\left(a\omega\sqrt{1-(\frac{x}{a})^2}\right) + \sigma dW \tag{3}$$

Where the parameter σ represents the strength of the stochastic noise. We can write the Fokker–Planck equation for this system, and without loss of generality we can for simplicity set $a = \omega = 1$ to obtain:

$$\partial_t P(x,t) = \partial_x(\sqrt{1-x^2}\cdot P(x,t)) + D\partial_{xx}P(x,t) \tag{4}$$

$$= \partial_x P(x,t)\sqrt{1-x^2} - P(x,t)\frac{x}{\sqrt{1-x^2}} + D\partial_{xx}P(x,t) \tag{5}$$

where $P(x,t)$ is the probability density function of the variable. We now look at the steady state ($\partial_t P(x,t) \approx 0$) and in the limit where $1 \gg D$. This represent the system with extremely low noise level, and we should be able to recognize a true oscillations above the Hopf bifurcation. Here our equation take the form:

$$\partial_x P(x)\sqrt{1-x^2} - P(x)\frac{x}{\sqrt{1-x^2}} = 0 \tag{6}$$

$$\Rightarrow \frac{x}{\sqrt{1-x^2}}dx = \frac{1}{P(x)}dP \tag{7}$$

$$\Rightarrow P(x) \propto \frac{1}{\sqrt{1-x^2}} \tag{8}$$

This distribution clearly has two singularities at $x = \pm 1$ (for $a = 1$), and in stochastic systems, this distribution will represent two separated peaks. We note that the existence of such peaks can be used to distinguish between DC's and SC's from $P(x)$, but this is only valid far above the Hopf bifurcation, since the peaks will "melt" together close to the bifurcation where $v(t)$ is no longer significantly larger than σ (Fig. 1C).

In this regime we apply time embedding, thereby turning the time series into polar coordinates where the radial component r, is the distance to the fixed point. A circular limit cycle is then a stable fixed point in r equal to the radius of the limit cycle (r^*). Assuming Gaussian noise (i.e. a Wiener process) in polar coordinates, the radial Langevin equation takes the form (see Appendix A):

$$dr = dt\left(f(r) + \frac{D}{r}\right) + \sqrt{2D}dW_r \tag{9}$$

where $f(r)$ is again the direction of the radial motion, similar to a force in an overdamped system. The Fokker Planck equation, in steady state where there is no dependency on t, describes the probability distribution $P(r)$ and takes the form:

$$-\left(f(r) + \frac{D}{r}\right)P(r) + D\partial_r P(r) = 0 \tag{10}$$

$$\Rightarrow \frac{1}{P(r)}dP = \left(\frac{f(r)}{D} + \frac{1}{r}\right)dr \tag{11}$$

$$\Rightarrow P(r) = Cre^{\frac{F(r)}{D}} \tag{12}$$

Here C is a normalization constant and $F(r)$ is the antiderivative of $f(r)$. Note that we assume that $e^{F(r)} \mapsto 0$ for $r \mapsto \infty$, since we consider a physical system that does not diverge to ∞, since otherwise the system would not have a well defined probability distribution in steady state.

Now differentiating this expression twice lead to the expression:

$$\frac{d^2P(r)}{dr^2} = Ce^{\frac{F(r)}{D}}\left(\frac{f(r)}{D} + \frac{1}{D}\partial_r(rf(r)) + r\frac{f(r)^2}{D^2}\right) \tag{13}$$

Evaluating this for $r \approx 0$ and Taylor expanding to first order $f(r=\epsilon) \approx f(0) + f'(0)\epsilon$ we obtain:

$$\left.\frac{d^2P(r)}{dr^2}\right|_{r=\epsilon} \approx Ce^{\frac{F(\epsilon)}{D}}\left(\frac{f'(0)\epsilon}{D} + \frac{1}{D}\partial_r(r^2f'(0))\Big|_{r=\epsilon} + \epsilon^3\frac{f'(0)^2}{D^2}\right) \tag{14}$$

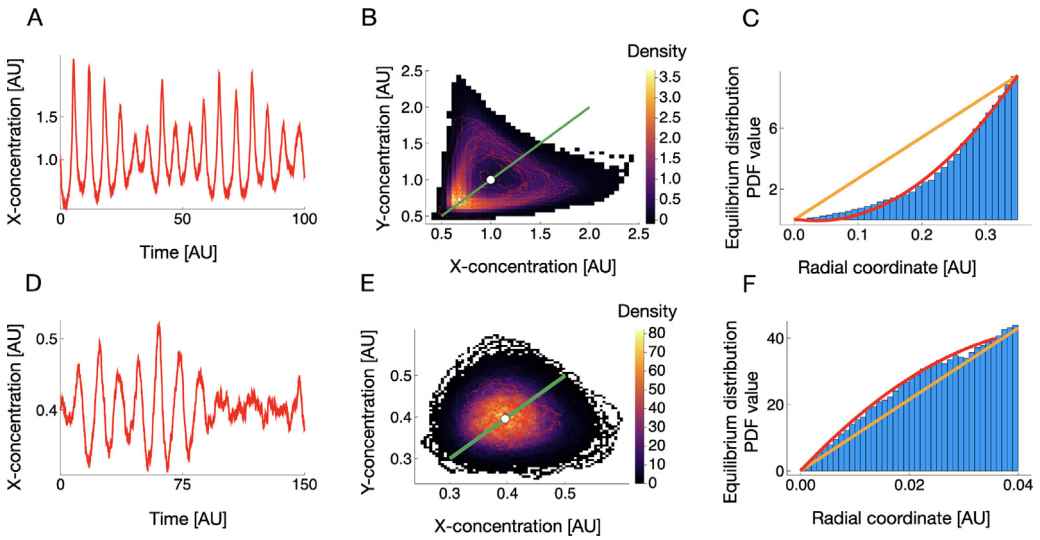

Fig. 2. Two examples of the proposed method. (A) Simulations of the Brusselator system with parameters $a = 1, b = 2.15, \sigma = 0.05$ (See Appendix B). (B) Distribution of $x(t), x(t+\tau)$ in two dimensions, of the time embedded data series for the data shown in (A). The white dots represent the fixed points. (C) Histogram of measured radial distribution of time embedded system ($P(r)$), The orange line is straight (second derivative=0), The red curve is fitted with a second order polynomial. (D) Simulations of the Glycolysis system model with parameters $a = 0.1, b = 0.4, \sigma = 0.01$ (See Appendix B). (E) Same as B, but for the Glycolysis system. (F) Same as C, but for the Glycolysis system.

Very close to the fixed point we keep only terms up to first order in ϵ leaving us with:

$$\left.\frac{d^2P(r)}{dr^2}\right|_{r=\epsilon} = \frac{3f'(r)}{D} C e^{\frac{F(r)}{D}} + \mathcal{O}(\epsilon^2) \propto f'(r) \tag{15}$$

Since the stochasticity constant, D, is always positive, this equation reveals the desired information about the distribution of radial positions of the system. Note that the only information we do know about $f(r)$ is that its first derivative is positive for unstable fixed points and negative for stable fixed points. The sign in the second derivative of the steady state probability distribution $P(r)$ is therefore only dependent on the stability of the fixed point. This means we can use the curvature of $P(r)$ as a test of whether the system is a DC or an SC and we can quantify our belief by the uncertainty in the fit.

Based on this we will apply the theoretical framework to simulated data, and investigate how one can use this approach to determine whether simulated systems has a limit cycle or a stable fixed point.

3. Practical implementation using hypothesis testing

To use the proposed method on a system in practice, it boils down to calculating the probability distribution $P(r)$ and measure whether it is concave or convex, which is the third step in the proposed method. From a practical point of view, we calculate the second derivative of the distribution by fitting it close to $r = 0$ with a second order polynomial $P(r) = ar^2 + br$. In Fig. 2 the method is explained in steps:

- We use a one dimensional time series of arbitrary length as input (Fig. 2 A+D).
- We apply time embedding to the series, resulting in a two-dimensional space (Fig. 2 B+E),
- We transform all points to radial coordinates and measure the second derivative of the distribution for $P(r)$ (Fig. 1 C+F).

For the distribution around $r \approx 0$, we can compare it to a straight line and classify it as either a DC or SC dependent on the sign of the curvature.

To check the general validity of the above arguments, we investigate four two-dimensional oscillators (see Appendix B for details):

1. The normal form of the Hopf bifurcation
2. The Glycolysis oscillator,
3. The Chlorine oscillator
4. The Brusselator.

To minimize the number of parameters, we will in the remaining part of this paper define the oscillations in terms of two parameters:

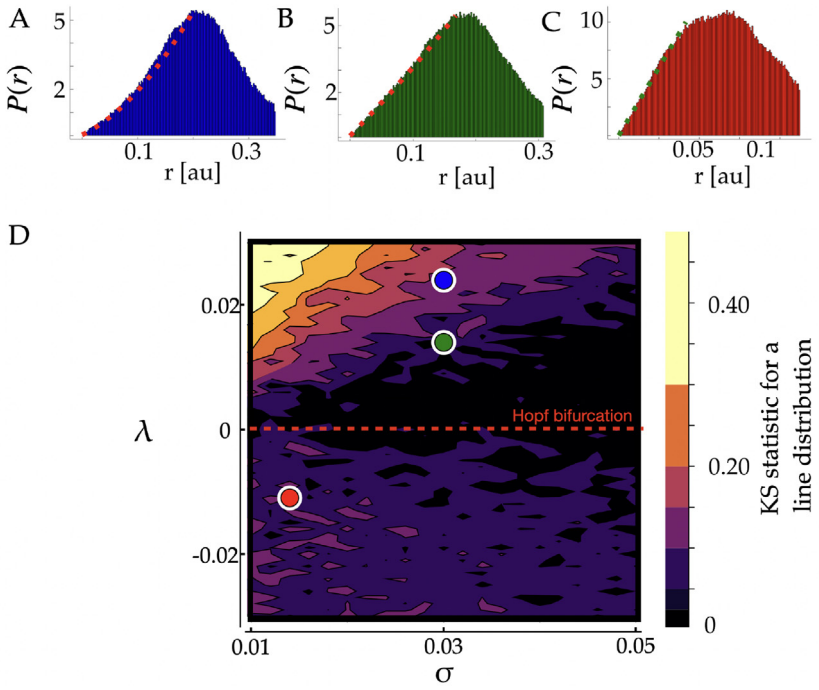

Fig. 3. (A) $P(r)$ as a function of r for $\lambda = 0.01$. Simulations made for the Glycolysis model with parameters $a = 0.1, b = 0.4, \sigma = 0.01$ (See Appendix B). (B) Same as A, but with $\lambda = 0.022$. (C) Same as A, but with $\lambda = -0.01$. (D) Kolmogorov Smirnov test statistic for a straight line distribution. The colours in the heatmap represents the KS statistics. Parameter values in λ and σ. Coloured dots correspond to A–C.

1. The bifurcation parameter λ which has the value $\lambda = 0$ at the Hopf bifurcation. For $\lambda > 0$ the system is a limit cycle (DC) (See Appendix B for details).
2. The noise parameter $\sigma = \sqrt{2D}$. This defines the strength of the applied white noise level and is the constant multiplied by a random number at each time step in the Langevin simulations.

We use these models, to test the concept by varying the values of λ. For $\lambda > 0$ the system is a DC, and for values where the repulsive force away from the fixed point dominates the stochastic fluctuations (i.e. $\lambda > \sigma$), it is possible to identify the curvature of $P(r)$ and reject the hypothesis of a straight line (Fig. 3A). For values $\lambda \approx 0$, where the stochastic level is comparable to the deterministic movement of the system, the curvature looks flat and it is not possible to reject neither hypothesis (Fig. 2B). Finally, if $\lambda < 0$, it is possible to extract the negative curvature of the distribution for the SC (Fig. 3C).

As a first test, we wanted to investigate how well these empirical curves differed from a straight line, that corresponds to the singular point of the Hopf bifurcation. Therefore we applied the one-sided Kolmogorov–Smirnov (KS) [40,41] test, to compare the empirical distribution with the reference distribution of a straight The KS test assumes as a null-hypothesis that the distributions are equal, and gives as output a probability to reject this, allowing us to make a hypothesis test (See Appendix C for further explanation). We obtained the test-statistic from the KS test and evaluated this for combinations of the Hopf parameter (λ) versus the stochastic parameter (σ) and visualized this as a heatmap (Fig. 3D). This heatmap visualize for what combinations of λ and σ we will be able to determine the second derivative of the distribution.

3.1. Dependency on the length of the time series

Since our method relies on results in equilibrium, it is clear that the longer the time series, the more certain is the result. With our method applied above, we investigate how many oscillations (or periods) are necessary to identify the underlying nature of the oscillations correctly. We applied this scheme for six λ-values above and below the Hopf bifurcation, and typically after 100–300 periods, the oscillations had been identified correctly (Fig. 4A). When comparing the time series by eye, it can otherwise be very difficult to distinguish a DC (Fig. 4B) from an SC (Fig. 4C), but using this our proposed method it relatively quickly becomes clear. We repeated the method for a doubled noise level, and found similar results in general, but where some of the DC simulations were more difficult to determine (Fig. 3d). Representative time series for this noise level is also shown for the DC (Fig. 4E) and the SC (Fig. 4F). We note that for the SC simulations (red, green and orange in Fig. 4A+D) the method correctly gives low probability for the dynamics to be a DC after approximately 250 oscillations. We want to stress, that since it is an equilibrium measure, these oscillations can also be gathered from multiple cells, if they are measured under the same conditions.

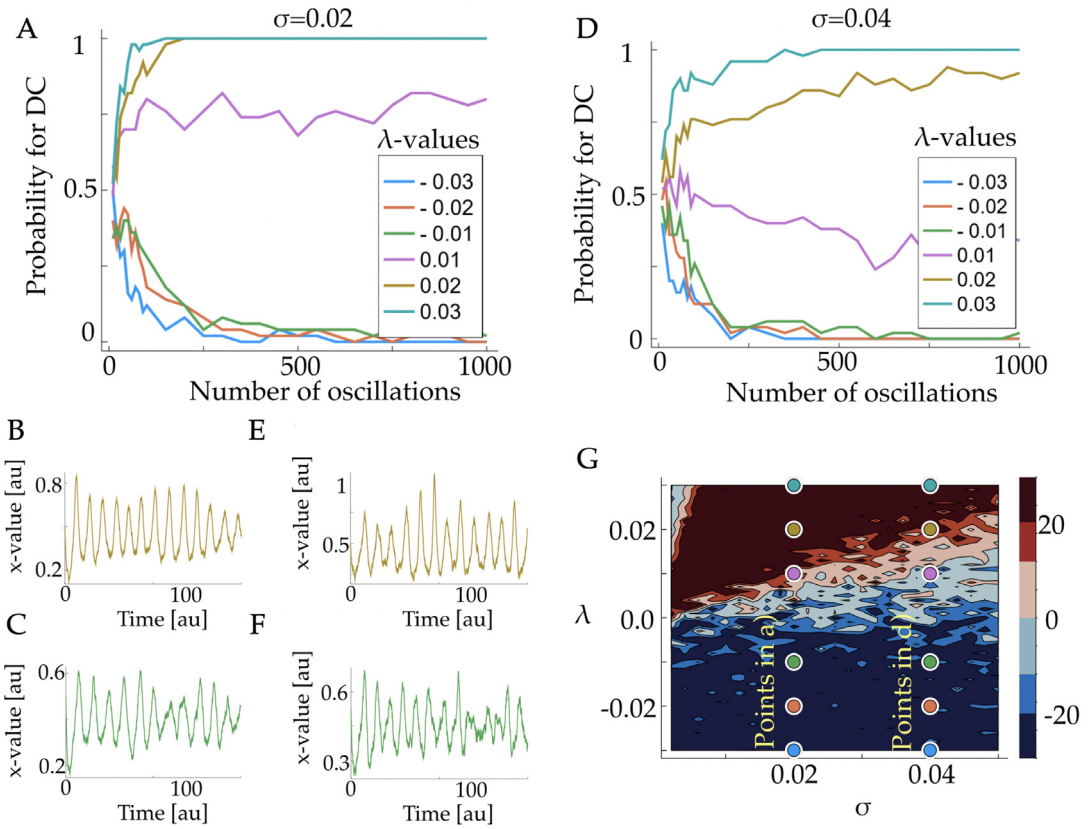

Fig. 4. (a) Probability for the time signal to be a DC evaluated after an increasing number of oscillating periods. Colours correspond to different values of λ. Noise level, $\sigma = 0.02$. (b) Representative trace for $\lambda = 0.02$ (c) Representative trace for $\lambda = -0.01$ (d–f) same as a–c but for $\sigma = 0.04$. (g) Heatmap showing a/σ_a for different combinations of parameters, it is the same underlying simulations of the Glycolysis oscillator as Fig. 3. Coloured dots correspond to lines in a+d.

Finally we tested the significance of the curvature parameter by fitting a second degree polynomial to the distribution for a large range of parameter combinations of λ and σ. In this procedure, we obtain a fitted value of the curvature parameter, a_{best} and an uncertainty in the parameter, σ_a. Taking the ratio of these two numbers, gives a measure of the significance of this parameter (i.e. how far away it is from zero in terms of its standard deviation). We therefore extracted this ratio, and generated a heatmap of a_{best}/σ_a for the σ, λ-space is shown in Fig. 4G. The parameters for the curves in Fig. 4 A+D are shown as points in Fig. 4G. Note that the results are asymmetric around the Hopf bifurcation ($\lambda = 0$), showing that the method never defines a non-oscillatory system (SC) to be a DC. Therefore the method should be applied with the null-hypothesis that the observed data is not a DC. Assuming Gaussianity in the parameters, the measure a_{best}/σ_a gives a probability with which one can reject the hypothesis of whether the oscillatory data comes from an SC and use it to declare the existence of a deterministic limit cycle.

4. Discussion

Oscillations are often observed in dynamical systems, and provides an important finger print of the dynamical behaviours in parameter spaces for a long list of systems in physics, chemistry and biology. In this paper we have shown how to transform one-dimensional time series into a form where the theory of stochastic dynamical systems can be used. This is done through a time embedding technique, leading to a system where the equilibrium distribution of the radial component close to the fixed point changes at the Hopf bifurcation. The method gives a simple way of distinguishing between stochastic (SC) and deterministic (DC) cycles, by determining whether the empirical probability distribution $P(r)$ is concave or convex.

We note that in our derivations all calculations have been performed in the framework of additive Gaussian noise. If instead the noise is multiplicative, it can still be Taylor expanded around the same fixed points, and the calculations will still hold, since the signs will not change. Multiplicative noise can make the approximations worse away from the fixed points, but the measure of curvature for very small values of r can still be used, since we are just looking at the

sign of the curvature. Therefore these results are also valid for systems where we perform simulations using the Gillespie algorithm [42], which is a method often used in modelling biological systems.

A fundamental challenge for many systems, especially in the field of biology, is to measure the required number of oscillation periods, in order for the hypotheses to properly be distinguishable. As far as the requirements to use the method, it unsurprisingly depends on the noise level and how close to the Hopf bifurcation the system is. The closer to the bifurcation and the more noise in the system, the larger data series are needed. Here we note that this is one of the strengths of using the equilibrium distribution as a measure, since one can in theory gather the distribution, by combining series from many cells. Thus the input data does not have to be one long time series, but could be the sum of multiple independent series. Such an approach will therefore be possible for many systems, except for systems with large series variation where combining data series leads to problem, since each individual series is not representative for the same equilibrium distribution. In such a case it is necessary to normalize the data.

We believe that this paper presents a valuable tool in applying theoretical results to describe various different dynamical systems and applying them to experimental time series obtained from physical, biological and chemical systems. We outline a simple way to separate the two cases; deterministic (DC) and stochastic (SC) oscillating cycles. If the requirements are fulfilled, the method should be easy to use for biological data series, since both time embedding and identifying whether a distribution is concave or convex are relatively simple tasks. Since oscillations represent a ubiquitous type of dynamics, the method can significantly help to improve the modelling approaches in the future.

CRediT authorship contribution statement

Emil S. Martiny: Conceived the setup of the paper, Performed the simulations, Writing. **Mogens H. Jensen:** Conceived the setup of the paper, Writing. **Mathias S. Heltberg:** Conceived the setup of the paper, Writing.

Declaration of competing interest

The authors declare that they have no known competing financial interests or personal relationships that could have appeared to influence the work reported in this paper.

Data availability

No data was used for the research described in the article.

Acknowledgement

We are grateful to Namiko Mitarai for interesting discussions on the validity of the theoretical assumptions. All authors acknowledge support from the Danish Council for Independent Research and Danish National Research Foundation through StemPhys Center of Excellence, grant number DNRF116. MLH acknowledge funding from the Lundbeck Foundation grant R347-2020-2250. MHJ acknowledges support from the Independent Research Fund Denmark grant number 9040-00116B.

Code availability

All code used for the analysis is available at https://github.com/ESMartiny/StochasticHopfBifurcation. It is written in Julia [43].

Appendix A. Stochastic differential equation in polar coordinates

Let us assume we have a two-dimensional system of coupled ordinary differential equations, with stochastic Langevin noise. These take the form:

$$dX = (-\partial_x(f(x,y)))dt + \sqrt{2D}\cdot dW_1 \tag{16}$$

$$dY = (-\partial_y(f(x,y)))dt + \sqrt{2D}\cdot dW_2 \tag{17}$$

Here dW_i has the fundamental property that $dW_i \cdot dW_i = 1$ and $dW_i \cdot dW_j = 0$, since the noise is uncorrelated. The function $f(x,y)$ corresponds to a potential in an overdamped system. Now assuming radial symmetry so $f \mapsto f(r)$ we can change the coordinates so the equations take the form:

$$dX = (-\partial_r(f(r))\frac{x}{r})dt + \sqrt{2D}\cdot dW_1 \tag{18}$$

$$dY = (-\partial_r(f(r))\frac{y}{r})dt + \sqrt{2D}\cdot dW_2 \tag{19}$$

Now we apply Ito's lemma, which can be viewed as the stochastic counterpart to the chain rule of calculus. We derive the differential for $r(x, y)$:

$$dr = \dot{r}dt + \partial_x r dX + \partial_y r dY + \frac{1}{2}\Big(\partial_{xx} r dX dX + \partial_{yy} r dY dY + 2\partial_{xy} r dX dY\Big) \tag{20}$$

Since r has no time dependency $\dot{r} = 0$, the next two terms give:

$$(\partial_x r)dX + (\partial_y r)dY = \frac{x^2}{r^2}\partial_r f(r)dt + \frac{y^2}{r^2}\partial_r f(r)dt + \frac{x}{r}\sqrt{2D}dW_1 + \frac{x}{r}\sqrt{2D}dW_2 \tag{21}$$

$$= \partial_r f(r)dt + \sqrt{2D}\Big(cos(\theta)dW_1 + sin(\theta)dW_2\Big) \tag{22}$$

Finally we note that $dW_i dW_i = \begin{cases} dt \text{ if } i = j \\ 0 \text{ otherwise} \end{cases}$.

Now gathering terms and keeping only terms to first order in dt, we get:

$$\frac{1}{2}\Big(\partial_{xx} r dX dX + \partial_{yy} r dY dY + 2\partial_{xy} r dX dY\Big) = \frac{1}{2}\Big((\partial_{xx} r)2Ddt + (\partial_{xx} r)2Ddt\Big) + \mathcal{O}(dt^{\frac{3}{2}}) \tag{23}$$

$$= \frac{D}{r}dt + \mathcal{O}(dt^{\frac{3}{2}}) \tag{24}$$

where we in the last line used the fact that $\partial_{xx} r + \partial_{yy} r = \frac{1}{r}$.

Collecting all these terms, and keeping only terms in first order of dt, leaves us with:

$$dr = \partial_r f(r)dt + \sqrt{2D}\Big(cos(\theta)dW_1 + sin(\theta)dW_2\Big) + \frac{D}{r}dt \tag{25}$$

Since dW_1 and dW_2 are normally distributed variables, their sum is also a normally distributed variable. This has mean $\mu = 0$ and standard deviation $\sigma = \sqrt{2Dcos(\theta)^2 + 2Dsin(\theta)^2} = \sqrt{2D}$. We can therefore write as a new stochastic variable dW_r, allowing us to describe the radial component of the stochastic variable:

$$dr = dt\Big(\partial_r f(r) + \frac{D}{r}\Big)dt + \sqrt{2D}dW_r \tag{26}$$

This is the radial part of the description. Note that in two dimensions we can also obtain the angular (θ) part of the stochastic differential, by applying the same recipe as above and using $\partial_x \theta = \frac{-y}{r^2}$, $\partial_y \theta = \frac{x}{r^2}$, $\partial_{xx}\theta + \partial_{yy}\theta = 0$. Here we end up with:

$$d\theta = \sqrt{\frac{2D}{r}}dW_\theta \tag{27}$$

We observe that there is no dependency on the "force" $(f(r))$ and since this is the one we aim to obtain information about we will not use the angular part in this paper. In the normal form of a limit cycle, the radial part has the form in the deterministic system:

$$\frac{dr}{dt} = r - \mu r^3 \tag{28}$$

With the above description, the radial part in the stochastic version takes the form:

$$dr = dt\Big(r - \mu r^3 + \frac{D}{r}\Big) + \sqrt{2D}dW_r \tag{29}$$

The noteworthy part of this is the added deterministic term $\frac{D}{r}$ in the radial equation that behave like a pressure away from the fixed point.

Appendix B. Mathematical description of oscillators

In this work we have used 4 different mathematical systems of ordinary differential equations to simulate the oscillatory behaviour in the presence of noise. These are each described here:

- The normal form:

$$\dot{x} = x\mu - \omega y - (ax + yb)(x^2 + y^2) \tag{30}$$

$$\dot{y} = y\mu + \omega x - (ay - bx)(x^2 + y^2) \tag{31}$$

$$\mu = \lambda \tag{32}$$

- The Glycolysis oscillator [44], b is the bifurcation parameter:

$$\dot{x} = -x + ay + x^2 y \tag{33}$$
$$\dot{y} = b - ay - x^2 y \tag{34}$$
$$b^2 = \frac{1}{2}(1 - 2a - 2\lambda \pm \sqrt{4\lambda^2 + 1 - 8a - 4\lambda}) \tag{35}$$

- The Chlorine oscillator [45], b is the bifurcation parameter:

$$\dot{x} = a - x - \frac{4xy}{1 + x^2} \tag{36}$$
$$\dot{y} = bx(1 - \frac{y}{1 + x^2}) \tag{37}$$
$$b = -\frac{10\lambda}{a} - \frac{2a\lambda}{5} + \frac{3a}{5} - \frac{25}{a} \tag{38}$$

- The Brusselator [46], B is the bifurcation parameter:

$$\dot{x} = A + yx^2 - Bx - x \tag{39}$$
$$\dot{y} = Bx - yx^2 \tag{40}$$
$$B = 2\lambda + 1 + A^2 \tag{41}$$

We note that for all the models, we apply stochastic noise, by including a white noise term, through the Langevin formulation. In this way all models, will have a stochastic term, where the parameter σ specifies the level of the noise. Numerically, we include this in the simulations, by adding a stochastic term of the form: $\sigma * \sqrt{dt}\mathcal{R}$, where $\mathcal{R}$ is a random number following the unit gaussian.

Appendix C. One sided Kolmogorov–Smirnov test

The Kolmogorov–Smirnov test is a non-parametric test that gives a probability that an empirical distribution is similar to some underlying distribution. Using a null-hypothesis that the two distributions come from the same probability density function, the test calculates the maximal distance between the empirical density function and the cumulative distribution function of the reference distribution. Suppose we have n random numbers: $X_1, \ldots, X_n$. The empirical distribution function is defined as:

$$F_n(x) = \frac{1}{n} \sum_{1 \le j \le n} I\{X_i \le x\}$$

Translated this means, that the value for some value x, is the number of elements that are smaller than x. Note that the empirical distribution function takes values from [0; 1] and it increases stepwise in step heights of $\frac{1}{n}$. The largest distance between the empirical distribution function and the cumulative distribution function for the reference distribution is now expressed as:

$$D_n = sub_{x \in \mathbf{R}} |F_n(x) - F(x)]$$

Here the Glivenko–Cantelli theorem proves that for large n $D_n \mapsto 0$ and Kolmogorov took this further and derived the rate of convergence [41]. Using this Kolmogorov distribution, one can use that:

$$P(\sqrt{n} = \text{sub}_{x \in \mathbf{R}} |F_n(x) - F(x)] \le t)$$
$$\equiv H(t) = 1 - 2 \sum_{j=1}^{\infty} (-1)^{j-1} e^{-2j^2 t^2}$$

With this one can directly obtain the probability of any distribution is similar to an underlying distribution. Note that we do not need any assumption on the shape of the distributions since the result holds for any distribution.

References

[1] J.H. Levine, Y. Lin, M.B. Elowitz, Functional roles of pulsing in genetic circuits, Science 342 (6163) (2013) 1193–1200.
[2] D. Gonze, J. Halloy, A. Goldbeter, Robustness of circadian rhythms with respect to molecular noise, Proc. Natl. Acad. Sci. 99 (2) (2002) 673–678.
[3] A. Pikovsky, M. Rosenblum, J. Kurths, R.C. Hilborn, Synchronization: A universal concept in nonlinear science, Amer. J. Phys. 70 (6) (2002) 655.
[4] M. Heltberg, R.A. Kellogg, S. Krishna, S. Tay, M.H. Jensen, Noise induces hopping between NF-κB entrainment modes, Cell Syst. 3 (6) (2016) 532–539.e3.
[5] A. Woller, H. Duez, B. Staels, M. Lefranc, A mathematical model of the liver circadian clock linking feeding and fasting cycles to clock function, Cell Rep. 17 (4) (2016) 1087–1097.

[6] T.Y.-C. Tsai, Y.S. Choi, W. Ma, J.R. Pomerening, C. Tang, J.E. Ferrell, Robust, tunable biological oscillations from interlinked positive and negative feedback loops, Science 321 (5885) (2008) 126–129.
[7] A. Amon, M. Lefranc, Topological signature of deterministic chaos in short nonstationary signals from an optical parametric oscillator, Phys. Rev. Lett. 92 (9) (2004) http://dx.doi.org/10.1103/physrevlett.92.094101.
[8] N. Mitarai, U. Alon, M.H. Jensen, Entrainment of noise-induced and limit cycle oscillators under weak noise, Chaos 23 (2) (2013) 023125.
[9] D. Pierson, F. Moss, Detecting periodic unstable points in noisy chaotic and limit cycle attractors with applications to biology, Phys. Rev. Lett. 75 (11) (1995) 2124–2127.
[10] P. Schmelcher, F.K. Diakonos, Detecting unstable periodic orbits of chaotic dynamical systems, Phys. Rev. Lett. 78 (25) (1997) 4733–4736.
[11] A. Eldar, M.B. Elowitz, Functional roles for noise in genetic circuits, Nature 467 (7312) (2010) 167–173.
[12] M.B. Elowitz, S. Leibler, A synthetic oscillatory network of transcriptional regulators, Nature 403 (6767) (2000) 335–338.
[13] M.B. Elowitz, Stochastic gene expression in a single cell, Science 297 (5584) (2002) 1183–1186.
[14] M. Behar, D. Barken, S.L. Werner, A. Hoffmann, The dynamics of signaling as a pharmacological target, Cell 155 (2) (2013) 448–461.
[15] M. Cirit, C.-C. Wang, J.M. Haugh, Systematic quantification of negative feedback mechanisms in the extracellular signal-regulated kinase (ERK) signaling network, J. Biol. Chem. 285 (47) (2010) 36736–36744.
[16] N. Hao, E.K.O. Shea, Signal-dependent dynamics of transcription factor translocation controls gene expression, Nat. Struct. Mol. Biol. 19 (1) (2011) 31–39.
[17] J.J. Tyson, K.C. Chen, B. Novak, Sniffers, buzzers, toggles and blinkers: Dynamics of regulatory and signaling pathways in the cell, Curr. Opin. Cell Biol. 15 (2) (2003) 221–231.
[18] M. Ronen, R. Rosenberg, B.I. Shraiman, U. Alon, Assigning numbers to the arrows: Parameterizing a gene regulation network by using accurate expression kinetics, Proc. Natl. Acad. Sci. 99 (16) (2002) 10555–10560.
[19] S. Tay, J.J. Hughey, T.K. Lee, T. Lipniacki, S.R. Quake, M.W. Covert, Single-cell NF-κB dynamics reveal digital activation and analogue information processing, Nature 466 (7303) (2010) 267–271.
[20] M.L. Heltberg, S. Krishna, M.H. Jensen, On chaotic dynamics in transcription factors and the associated effects in differential gene regulation, Nature Commun. 10 (1) (2019) http://dx.doi.org/10.1038/s41467-018-07932-1.
[21] A. Hoffmann, The ikappa B-NF-κ B signaling module: Temporal control and selective gene activation, Science 298 (5596) (2002) 1241–1245.
[22] D.E. Nelson, Oscillations in NF-κB signaling control the dynamics of gene expression, Science 306 (5696) (2004) 704–708.
[23] M.H. Jensen, S. Krishna, Inducing phase-locking and chaos in cellular oscillators by modulating the driving stimuli, FEBS Lett. 586 (11) (2012) 1664–1668.
[24] S. Krishna, M.H. Jensen, K. Sneppen, Minimal model of spiky oscillations in NF-κB signaling, Proc. Natl. Acad. Sci. 103 (29) (2006) 10840–10845.
[25] N. Geva-Zatorsky, N. Rosenfeld, S. Itzkovitz, R. Milo, A. Sigal, E. Dekel, T. Yarnitzky, Y. Liron, P. Polak, G. Lahav, U. Alon, Oscillations and variability in the p53 system, Mol. Syst. Biol. 2 (1) (2006).
[26] M.L. Heltberg, S. hong Chen, A. Jiménez, A. Jambhekar, M.H. Jensen, G. Lahav, Inferring leading interactions in the p53/Mdm2/Mdmx circuit through live-cell imaging and modeling, Cell Syst. 9 (6) (2019) 548–558.e5.
[27] G. Lahav, N. Rosenfeld, A. Sigal, N. Geva-Zatorsky, A.J. Levine, M.B. Elowitz, U. Alon, Dynamics of the p53-Mdm2 feedback loop in individual cells, Nature Genet. 36 (2) (2004) 147–150.
[28] B. Mengel, A. Hunziker, L. Pedersen, A. Trusina, M.H. Jensen, S. Krishna, Modeling oscillatory control in NF-κB, p53 and Wnt signaling, Curr. Opin. Genet. Dev. 20 (6) (2010) 656–664.
[29] B. Øksendal, Stochastic Differential Equations: An Introduction with Applications, sixth ed., Springer-Verlag GmbH, 2013.
[30] H. Leung, Stochastic Hopf bifurcation in a biased van der Pol model, Physica A 254 (1–2) (1998) 146–155.
[31] I. Bashkirtseva, L. Ryashko, H. Schurz, Analysis of noise-induced transitions for Hopf system with additive and multiplicative random disturbances, Chaos Solitons Fractals 39 (1) (2009) 72–82.
[32] P.H. Baxendale, A stochastic Hopf bifurcation, Probab. Theory Relat. Fields 99 (1994) 581–616.
[33] K. Schenk-Hoppé, Stochastic Hopf bifurcation: An example, Int. J. Non-Linear Mech. 31 (5) (1996) 685–692.
[34] L. Arnold, N.S. Namachchivaya, K.R. Schenk-HoppÉ, Toward an understanding of stochastic Hopf bifurcation, Int. J. Bifurcation Chaos 06 (11) (1996) 1947–1975.
[35] L. Arnold, Bifurcation theory, in: Springer Monographs in Mathematics, Springer Berlin Heidelberg, 1998, pp. 465–531.
[36] S.-h. Chen, W. Forrester, G. Lahav, Schedule-dependent interaction between anticancer treatments, Science 351 (6278) (2016) 1204–1208, URL https://science.sciencemag.org/content/351/6278/1204.
[37] A.J. McKane, T.J. Newman, Predator-prey cycles from resonant amplification of demographic stochasticity, Phys. Rev. Lett. 94 (21) (2005) 218102.
[38] A.J. McKane, J.D. Nagy, T.J. Newman, M.O. Stefanini, Amplified biochemical oscillations in cellular systems, J. Stat. Phys. 128 (1) (2007) 165–191.
[39] H.D. Abarbanel, J.P. Gollub, Analysis of observed chaotic data, Phys. Today 49 (11) (1996) 86.
[40] Barlow, Statistics, John Wiley & Sons, 1993.
[41] J. Vrbik, Deriving cdf of Kolmogorov-Smirnov test statistic, Appl. Math. 11 (3) (2020) 227–246.
[42] D.T. Gillespie, Exact stochastic simulation of coupled chemical reactions, J. Phys. Chem. 81 (25) (1977) 2340–2361.
[43] J. Bezanson, A. Edelman, S. Karpinski, V.B. Shah, Julia: A fresh approach to numerical computing, SIAM Rev. 59 (1) (2017) 65–98.
[44] A. Goldbeter, M.J. Berridge, Oscillatory enzymes: Simple periodic behaviour in an allosteric model for glycolytic oscillations, in: Biochemical Oscillations and Cellular Rhythms: The Molecular Bases of Periodic and Chaotic Behaviour, Cambridge University Press, 1996, pp. 31–88.
[45] I. Lengyel, G. Rábai, I.R. Epstein, Experimental and modeling study of oscillations in the chlorine dioxide-iodine-malonic acid reaction, 1990.
[46] A. Nandi, B. Lindner, Intrinsic common noise in a system of two coupled brusselators, Chem. Phys. 375 (2) (2010) 348–358, Stochastic processes in Physics and Chemistry (in honor of Peter Hänggi).